Theoretical Studies of Dissociative Phosphoryl Transfer in Interconversion of Phosphoenolpyruvate to Phosphonopyruvate: Solvent Effects, Thio Effects, and Implications for Enzymatic Reactions

Dingguo Xu,[†] **Hua Guo,**[*,†] **Yun Liu,**[‡] **and Darrin M. York**[*,‡]

Department of Chemistry, University of New Mexico, Albuquerque, New Mexico 87131, and Department of Chemistry, University of Minnesota, Minneapolis, Minnesota 55455

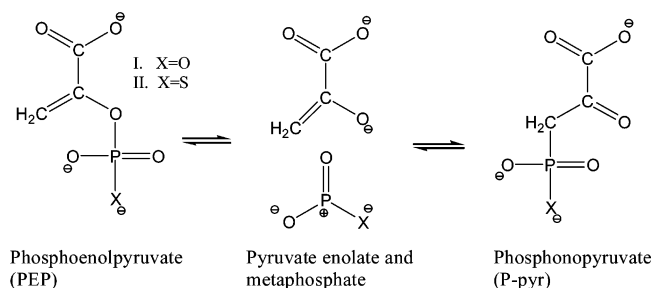*Received: March 1, 2005; In Final Form: May 11, 2005*

The conversion of phosphoenolpyruvate (PEP) to phosphonopyruvate (P-pyr) is catalyzed by PEP mutase via a dissociative mechanism. In this work, we investigate the uncatalyzed reaction using ab initio methods, density functional theory, and the semiempirical MNDO/d method. Comparisons of geometries and relative energies of stationary points (minima and transition states) with density functional results indicate that the semiempirical method is reasonably accurate. Solvent effects are examined using implicit solvent models, including the recently extended smooth conductor-like screening model. Due to the large negative charge carried by the system, solvation is found to drastically alter the location and energy of stationary points along the dissociative reaction pathways. The influence of substituting a nonbridging phosphoryl oxygen by sulfur (thio effects) was also investigated. Implications of these results for the enzymatic reaction are discussed.

I. Introduction

The transfer of the phosphoryl group plays a central role in many biochemical processes, such as energy conversion and cell signaling.[1,2] As a result, phosphoryl transfer reactions have been extensively studied in both solution[3−5] and enzymatic systems.[6−8] There are three limiting-case mechanisms that differ in the relative timing of the nucleophilic addition (NA) and elimination (E) steps. The concerted mechanism is characterized by a bipyramidal transition state formed by synchronous NA and E steps, while the stepwise associative mechanism features a pentacoordinate phosphorane intermediate flanked by the transition states for the NA and E steps. In the dissociative mechanism, the metaphosphate (PO_3^-) intermediate is first formed and subsequently reacts with the nucleophile. The particular mechanistic pathway that a phosphoryl transfer reaction adopts depends on many factors such as nucleophile strength, leaving group mobility, protonation state, interaction with metal ions, and solvation.

The prevailing mechanism in the solution-phase phosphoryl transfer reactions involving phosphate monoesters is an intermediate case between the dissociative and the concerted limits, featuring a metaphosphate-like transition state with significant bond cleavage to the leaving group and little bond formation with the nucleophile.[4,7] The dominance of the dissociation mechanism has recently been called into question by Florian and Warshel,[9] whose theoretical calculations suggested similar barrier heights for both associative and dissociative reaction pathways. However, subsequent theoretical investigations pointed out the importance of solvent water in assisting the reaction,[10−13] reaffirming the preference for the dissociative mechanism. For phosphate diesters and triesters, however, the associative mechanism is thought to be more prevalent.[7]

* Authors to whom correspondence should be addressed. E-mail: hguo@unm.edu; york@chem.umn.edu.
† University of New Mexico.
‡ University of Minnesota.

SCHEME 1: Proposed Mechanism for Interconversion of PEP to P-pyr Catalyzed by PEP Mutase

Phosphoenolpyruvate (PEP)   Pyruvate enolate and metaphosphate   Phosphonopyruvate (P-pyr)

It has been argued that the dissociative transition state is difficult to be changed by the environment.[14,15] Indeed, many examples of a dissociative transition state have been reported for enzyme-catalyzed phosphoryl transfer reactions.[7,16,17] However, few have been shown to proceed via a fully dissociative mechanism, producing the metaphosphate intermediate.[8,18] One such example is phosphoenolpyruvate (PEP) mutase, which catalyzes the transfer of the phosphoryl group from O in PEP to C (Scheme 1), producing phosphonopyruvate (P-pyr).[19−21] It is one of the most extensively studied enzymes in the biosynthesis pathway of phosphonates,[22] which feature a covalent P−C linkage and are thought to predate earth's oxygen-rich atmosphere.[23] Very recently, structures of free PEP mutase and its complexes with several inhibitors have been determined by X-ray diffraction.[24,25] In combination with kinetic and mutagenesis data,[26−29] the phosphoryl transfer mechanism was identified as a dissociative one involving the metaphosphate intermediate.[25] This conclusion is primarily based on the failure to locate the putative nucleophile by exhaustive site-directed mutations of active-site residues and the X-ray structure of the enzyme complexed with a P-pyr analogue.[25] Such a dissociation mechanism is also consistent with the retention of the configuration observed in this enzymatic reaction.[21,30]

While the structural and kinetic data supply essential insights, they are not detailed enough to provide complete microscopic characterization of the enzymatic reaction. Theoretical studies, however, offer complementary perspectives that may aid our understanding of the reaction mechanism and catalysis strategy.[31,32] A particularly effective approach to study enzymatic reactions is the quantum mechanical/molecular mechanical (QM/MM) method,[33-36] which divides the system into a QM zone surrounded by a MM region. QM/MM simulations of phosphoryl transfer reactions such as the one catalyzed by PEP mutase are particularly challenging for two main reasons: First, the involvement of d-orbitals in phosphorus renders the commonly used semiempirical QM methods such as AM1 and PM3 unsuitable.[37,38] Second, the anionic nature of the substrate demands an accurate treatment of long-range electrostatic interactions and solvent effects.[9,39-44] The solvent effect is expected to be particularly significant for the current system because PEP carries three negative charges in the range of physiological pH. As a result, an enzymatic or solvent environment is likely to significantly shift the location of stationary points along the reaction coordinate relative to those in the gas phase.

To provide a reference point for studying the rearrangement of PEP to P-pyr catalyzed by this important and unique enzyme, we report in this work ab initio, density functional theory, and semiempirical MNDO/d investigations of the uncatalyzed reaction in both the gas phase and aqueous solution. Mechanistic studies can also be aided by substitution of a nonbridging oxygen in the phosphoryl group with sulfur. This so-called "thio effect"[45,46] is thus investigated in both gas and aqueous phases as well. In addition, this work has two other objectives. First, we hope to understand the effect of solvation on the model reaction, which has not been studied before and may shed light on other solution-phase phosphoryl transfer reactions. The solvation is modeled with implicit solvent models, including the polarized continuum model (PCM)[47,48] and the conductor-like screening model (COSMO).[49] Second, we would like to further test a newly developed QM solvation model for treating biological phosphate systems, which is based on the MNDO/d[37] method and the recently proposed smooth COSMO (SCOSMO).[50] The validity of the MNDO/d-SCOSMO approach, which has recently been implemented in CHARMM[51] and tested for some biologically relevant systems,[52] is important for an accurate QM/MM study of the enzymatic system. This work is organized as follows. The computational methods used in the calculations are briefly discussed in section II. The results are presented and discussed in section III. The conclusions are given in section IV.

II. Theory

As depicted in Scheme 1, the phosphoryl group transfer reaction involves the cleavage of a P-O bond and the formation of a P-C bond via the pyruvate enolate-metaphosphate intermediate, without the participation of a nucleophile. Our calculations thus focused on reactions along these two bonds. The phosphate group is treated as a dianion, which is the dominant form at physiological pH (7.5).[53,54] The participation of solvent water as a proton-transfer catalyst is not considered in this work. The total charge of the system is thus -3. The atom definitions are given in Chart 1.

Both ab initio and density functional theory (DFT) calculations were carried out using the Gaussian 03 suite of programs.[55] In DFT optimization, the B3LYP (Becke-3 exchange[56] and Lee-Yang-Parr correlation[57]) functional and the 6-31++G-(d,p) basis set were used. The diffuse functions are known to

CHART 1: Atomic Definitions

I. X=O
II. X=S
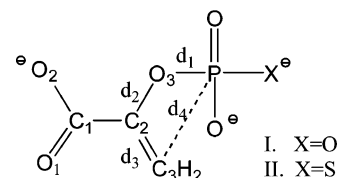
be important for anionic species. Single-point B3LYP calculations with the 6-311++G(3df,2p) basis set were then performed at these stationary points. The latter was used to conform with the protocol in our earlier work on biologically important phosphorus compounds.[44,58] The stationary points were also determined for the native reactions by the restricted Hartree-Fock (HF) theory using the 6-31++G(d,p) basis set. The electron correlation was then included via second-order Møller-Plesset (MP2) calculations at the HF geometries using the 6-311++G(3df,2p) basis set.

The stationary points corresponding to the reactant, product, and transition states were further confirmed by additional frequency calculations, and their connectivity was established by intrinsic reaction coordinate (IRC) calculations.[59,60] The free energy of the system can be obtained using standard statistical formulas. The intermediate, consisting of the metaphosphate anion (PO_3^-) and pyruvate enolate, was considered in two separate calculations for the two species. The energy and other thermodynamic properties were thus obtained simply as the summation of these two parts.

As mentioned earlier, the large negative charge carried by the PEP system is expected to induce substantial solvent polarization. For the DFT calculations, the solvent effects were taken into consideration using implicit solvent models, namely, PCM[47,48] and COSMO.[49] But as shown below, single-point PCM/COSMO calculations based on the gas-phase stationary points do not reflect the change of solute geometry induced by solvation that in some cases can lead to considerable error. Ideally, optimization of the solute should incorporate the solvent effects, as done in the SCOSMO approach[50] or using explicit solvents.[43,61,62] Although many implicit solvent models are capable of computing derivatives, such optimizations are usually unstable due to the fact that the derivatives are not rigorously smooth functions of the nuclear coordinates. In this work, we employed a constrained optimization approach to examine the effects of solvent on the location and energy of stationary points along the reaction coordinate. To this end, the minimal energy path along one of the two bond coordinates ($P-O_3$ and $P-C_3$) was first obtained in the gas phase. PCM calculations were then performed for all the points along the minimal energy path, and the stationary points of the solvated solute were approximated by the minima and maxima of the resulting energy curve. In all of the PCM calculations, the UAKS radii[63] implemented in Gaussian 03 were used.

The semiempirical calculations were performed using the MNDO/d method implemented in MNDO97.[37] The MNDO/d method is a reparametrization of the MNDO model with a Hamiltonian that includes d-orbitals. As a result, it yields a much better description of systems containing third row elements such as sulfur and phosphorus. The solvation is treated with the newly proposed SCOSMO method,[50-52] as implemented in MNDO97. Thanks to its ability to calculate analytic derivatives, the SCOSMO approach allows the explicit geometry optimization of solvated species. In the SCOSMO/MNDO/d calculations, the Bondi atomic radii[64] were used.

Studies of Dissociative Phosporyl Transfer

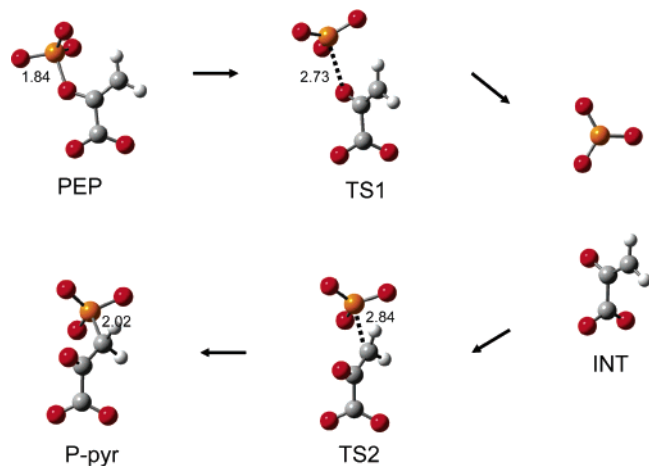*J. Phys. Chem. B, Vol. 109, No. 28, 2005* **13829**

Figure 1. Stationary points for the gas-phase interconversion of PEP to P-pyr via the pyruvate enolate−metaphosphate intermediate obtained at the B3LYP/6-31++G(d,p) level of theory.
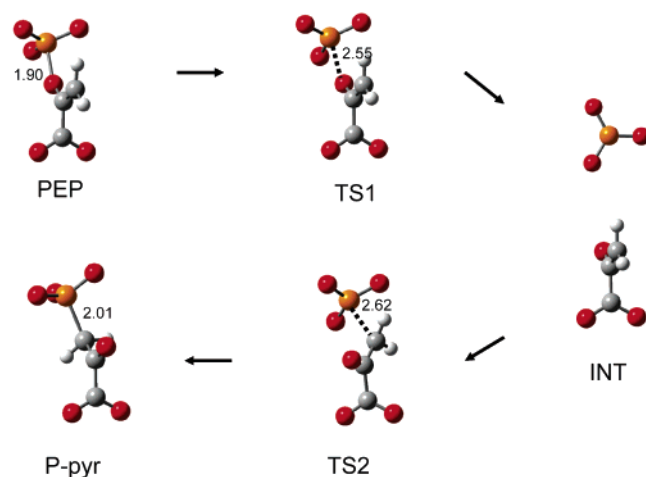

Figure 2. Stationary points for the gas-phase interconversion of PEP to P-pyr via the pyruvate enolate−metaphosphate intermediate obtained at the MNDO/d level of theory.

III. Results

A. Gas-Phase Reactions. Optimized geometries of stationary points for the gas-phase phosphoryl transfer reaction from PEP to P-pyr via the pyruvate enolate−metaphosphate intermediate are displayed in Figures 1 and 2 for B3LYP and MNDO/d calculations, respectively. The P−O_3 or P−C_3 bond length is also indicated in the figures. The geometries obtained from the HF optimizations are quite similar and thus not displayed. The energetics and key geometric parameters of these stationary points are collected in Tables 1 and 2. Unless stated otherwise,
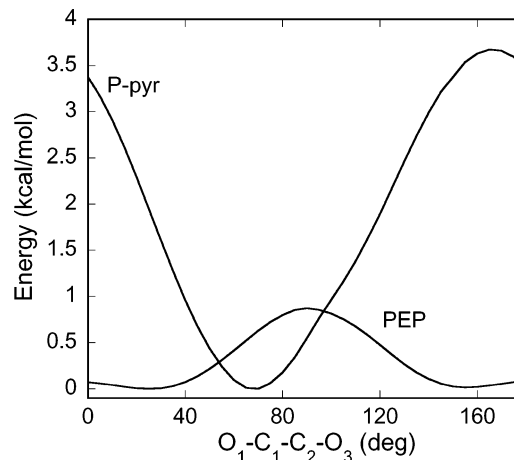

Figure 3. Minimal energy potential along the O_1−C_1−C_2−O_3 dihedral angle for both PEP and P-pyr.

the results quoted below are from single-point B3LYP calculations with the 6-311++G(3df,2p) basis set at the geometry optimized with the 6-31++G(d,p) basis set.

PEP is considered as a "high-energy" molecule because of its large exothermicity in hydrolysis. Its structure has been studied theoretically previously but at a much lower level of theory.[65,66] As shown in Table 2, the equilibrium geometry of PEP obtained from the DFT and HF calculations is in general agreement and also similar to earlier theoretical results.[65,66] However, the P−O_3 bond length obtained from the HF calculation is slightly shorter than the B3LYP value. Both HF and B3LYP calculations predict that the enol and carboxylate groups are twisted out of planarity, with an O_1−C_1−C_2−O_3 dihedral angle of 144.1° and 156.1°, respectively. The nonplanarity of the enolpyruvyl group has been observed in X-ray diffraction studies, and the dihedral angle depends sensitively on the protonation state and the environment.[67−70] To understand the conformational energetics for PEP, we have computed the minimal energy path along the O_1−C_1−C_2−O_3 dihedral angle. As shown in Figure 3, the rotation along the C_1−C_2 bond is quite free.

The cleavage of the P−O_3 bond in PEP in the gas phase is an activated process, and the energy barrier is calculated to be 8.75 and 14.17 kcal/mol at the B3LYP and MP2 levels, respectively. However, it releases ∼100 kcal/mol of energy, which can be largely attributable to the Coulomb repulsion between the two negatively charged products. The corresponding transition state (TS1) has an imaginary frequency of 84.67 cm^{-1} at the B3LYP level along the reaction coordinate consisting primarily of the P−O_3 bond, which is significantly elongated to 2.73 Å from the equilibrium value of 1.84 Å. It is interesting

TABLE 1: Energetics for Interconversion of PEP to P-pyr via the Pyruvate Enolate−Metaphosphate Intermediate (INT)[a]

method	PEP	TS1	INT	TS2	P-pyr
$\Delta E_{\text{gas(B3LYP/6-31+G(d,p))}}$	0.0	8.75	−103.6	5.76	−1.55
$\Delta E_{\text{gas(B3LYP/6-31++G(d,p))}}$	0.0	8.73	−103.8	5.66	−1.62
$\Delta E_{\text{gas(B3LYP/6-311++G(3df,2p)//B3LYP/6-31++G(d,p))}}$	0.0	8.75	−105.2	6.67	0.79
$\Delta E_{\text{gas(MP2/6-311++G(3df,2p)//HF/6-31++G(d,p))}}$	0.0	14.17	−97.90	12.78	1.75
$\Delta G_{\text{gas(B3LYP/6-311++G(3df,2p)//B3LYP/6-31++G(d,p))}}$	0.0	5.51	−119.2	4.50	1.16
$\Delta G_{\text{gas}} + \Delta G_{\text{solv(PCM)}}$ (single-point)	0.0	12.92	−5.89	15.05	3.67
$\Delta G_{\text{gas}} + \Delta G_{\text{solv(COSMO)}}$ (single-point)	0.0	11.04	−5.85	14.47	3.64
$\Delta E_{\text{opt(PCM)}}$ (estimated from Figure 4)	0.0	22.68		19.11	−0.61
$\Delta E_{\text{gas(MNDO/d)}}$	0.0	5.89	−110.79	12.52	2.17
$\Delta G_{\text{gas(MNDO/d)}}$	0.0	4.90	−122.43	12.03	1.96
$\Delta E_{\text{opt(SCOSMO/MNDO/d)}}$	0.0	21.11	19.18	24.43	1.57
$\Delta G_{\text{opt(SCOSMO/MNDO/d)}}$	0.0	18.56	6.91	23.66	1.90

[a] Energy units are given in kcal/mol.

TABLE 2: Geometries of Stationary Points for Interconversion of PEP to P-pyr[a]

method	d_1	d_2	d_3	d_4	φ[b]
		PEP			
B3LYP/6-31++G(d,p)	1.8431	1.3330	1.3643	3.3014	156.1
HF/6-31++G(d,p)	1.7611	1.3164	1.3440	3.2588	144.1
MNDO/d	1.9005	1.3070	1.3777	3.6686	91.9
SCOSMO/MNDO/d	1.7619	1.3578	1.3547	3.6978	65.9
		TS1			
B3LYP/6-31++G(d,p)	2.7272	1.2873	1.3960	4.2334	114.1
HF/6-31++G(d,p)	2.6067	1.2638	1.3857	4.2273	90.2
MNDO/d	2.5520	1.2731	1.3967	4.4509	91.3
SCOSMO/MNDO/d	2.9491	1.2864	1.3744	5.1841	65.2
		TS2			
B3LYP/6-31++G(d,p)	4.7507	1.2759	1.4248	2.8440	72.1
HF/6-31++G(d,p)	4.6474	1.2482	1.4215	2.7696	75.1
MNDO/d	4.3854	1.2602	1.4356	2.6226	81.7
SCOSMO/MNDO/d	4.3262	1.2677	1.4032	2.6905	99.9
		P-pyr			
B3LYP/6-31++G(d,p)	3.8601	1.2461	1.4933	2.0207	68.2
HF/6-31++G(d,p)	3.7156	1.2134	1.5082	1.9387	69.3
MNDO/d	3.5543	1.2346	1.5236	2.0125	87.2
SCOSMO/MNDO/d	3.6002	1.2336	1.5190	1.9219	110.3

[a] Bond lengths are given in angstroms, and angles are given in degrees. [b] φ is defined as the $O_1-C_1-C_2-O_3$ dihedral angle.

to note that the $O_1-C_1-C_2-O_3$ dihedral angle is reduced to 114.1° at the transition state, featuring near perpendicular enol and carboxylate planes. Similar changes were found in the HF geometries as well. As shown in Table 2, other geometric changes include a shortened C_2-O_3 bond and elongated C_2-C_3 bond, reflecting the changing bonding characteristics.

The geometries of the MNDO/d stationary points are similar to the B3LYP and HF ones discussed above. For example, the $P-O_3$ bond increases from 1.90 Å at the PEP equilibrium to 2.55 Å at the transition state (TS1). This is accompanied by other geometric changes highlighted in Table 2. The most pronounced difference from the B3LYP and HF results is perhaps the $O_1-C_1-C_2-O_3$ dihedral angle, which is almost the same for PEP and TS1, 91.9° and 91.3°, respectively. While the agreement is reasonable at the transition state, the near perpendicular enol and carboxylate planes in PEP are clearly an artifact of the MNDO/d model. However, as discussed below, the rotational barrier about the C_1-C_2 bond is quite small. From Table 1, it is readily seen that the barrier height (5.89 kcal/mol) and dissociation energy (−110.79 kcal/mol) are also in keeping with the DFT and HF results, although MNDO/d seems to underestimate the activation energy.

The HF, B3LYP, and MNDO/d methods all found the metaphosphate with the D_{3h} symmetry, and the P−O bond length is 1.47, 1.51, and 1.50 Å, respectively. In addition, the pyruvate enolate was found to feature near perpendicular enol and carboxylate planes, with the $O_1-C_1-C_2-O_3$ dihedral angle of 89.5°, 93.8° and 90.0°, respectively. At the MNDO/d level, a planar geometry also exists at a slightly lower energy, which is again considered as an artifact of the semiempirical model. In pyruvate enolate, both the C_3 and the O_3 atoms carry significant negative charges, which are −0.37e (−0.56e) and −0.69e (−0.81e) at the B3LYP (HF) level, respectively, making them effective nucleophiles for reconnecting with the phosphate group.

The dissociation of P-pyr also has a barrier (TS2), whose height is 11.03, 5.88, and 10.35 kcal/mol from the MP2, B3LYP, and MNDO/d models, respectively. The energies of P-pyr and TS2 are sensitive to the basis set used in the calculation, as shown in Table 1. The geometries of the corresponding

stationary points are also included in Figures 1 and 2 and listed in Table 2. In the B3LYP calculations, for example, the transition state for the $P-C_3$ bond cleavage features an elongated $P-C_3$ bond (2.84 Å) versus the equilibrium value of 2.02 Å. A similar trend is observed in the HF calculations, although the corresponding $P-C_3$ bond length is somewhat shorter. But unlike the dissociation of PEP, the $O_1-C_1-C_2-O_3$ dihedral angle from the B3LYP calculations hardly changes from the P-pyr (68.2°) to TS2 (72.1°). The corresponding values for HF (69.3° and 75.1°) and for MNDO/d (87.2° and 81.7°) are quite close. In Figure 3, we also include the minimal energy potential for P-pyr along the dihedral angle. The height of the barrier is only about 3.5 kcal/mol. Interestingly, both planar[66,71] and nonplanar P-pyr geometries[25] have been reported in crystal and enzymatic environments. Given the highly charged nature of the species, we believe that the observed planar conformation is due to strong electrostatic interaction of P-pyr with its environment.

B. Solvent Effects. As a first step, the solvent effects were investigated by single-point PCM and COSMO calculations based on gas-phase optimized DFT geometries. As shown in Table 1, the solvation raises the PEP dissociation barrier (TS1) by ∼7 kcal/mol and the P-pyr dissociation barrier (TS2) by ∼8 kcal/mol. These changes are respectable but are smaller than that found for the similar P−O bond cleavage of methyl phosphate (∼20 kcal/mol).[52] This is likely due to the smaller size of methyl phosphate relative to PEP.

The loose transition states with small imaginary frequencies and their anionic nature render them susceptible to solvent-induced geometric changes. To demonstrate this point, we carried out PCM calculations along the gas-phase minimal energy paths at the B3LYP/6-31+G(d,p) level for the two reaction coordinates, which are defined as the $P-O_3$ and $P-C_3$ distances for the dissociation of PEP and P-pyr, respectively. Approximately 50 points with a step size of 0.05 Å were computed for each dissociation process. In Figure 4, the total energy, which consists of both the electronic and the solvation energies, is plotted as a function of the reaction coordinates. Comparisons with the gas-phase curves clearly show that solvation drastically alters the position and energy of the stationary points. For instance, the $P-O_3$ bond length is shortened by 0.1 Å for the PEP in solution, while elongated by 0.85 Å at the transition state for its dissociation. Similar shifts of the $P-C_3$ bond (0.1 and 0.5 Å) were also observed for the dissociation of P-pyr. At the same time, the barrier is increased to 22.7 and 19.7 kcal/mol for the dissociation of PEP and P-pyr, respectively. Admittedly, these results should not be viewed as quantitative because the gas-phase structures were not allowed to relax in solution. The lack of self-consistency is apparently responsible for the spikes in the energy curves of the solvated systems. Nonetheless, they clearly demonstrated the danger in estimating solvent effects by using geometries of gas-phase stationary points.

Although direct and efficient geometry optimization of solvated species is still difficult with ab initio and DFT methods, the newly developed SCOSMO method[50] allows such optimization within the framework of the MNDO/d method.[51,52] Figure 5 displays the optimized structures obtained using the SCOSMO/MNDO/d approach. In comparison with the gas-phase stationary points, the solvent-induced geometric changes are apparent. For example, the $P-O_3$ bond is shortened by 0.14 Å to 1.76 Å for PEP, while elongated by 0.40 Å to 2.95 Å at TS1. The changes are less dramatic for the dissociation of P-pyr; the $P-C_3$ bond is shortened by 0.09 Å to 1.92 Å for P-pyr, while elongated by

Studies of Dissociative Phosporyl Transfer

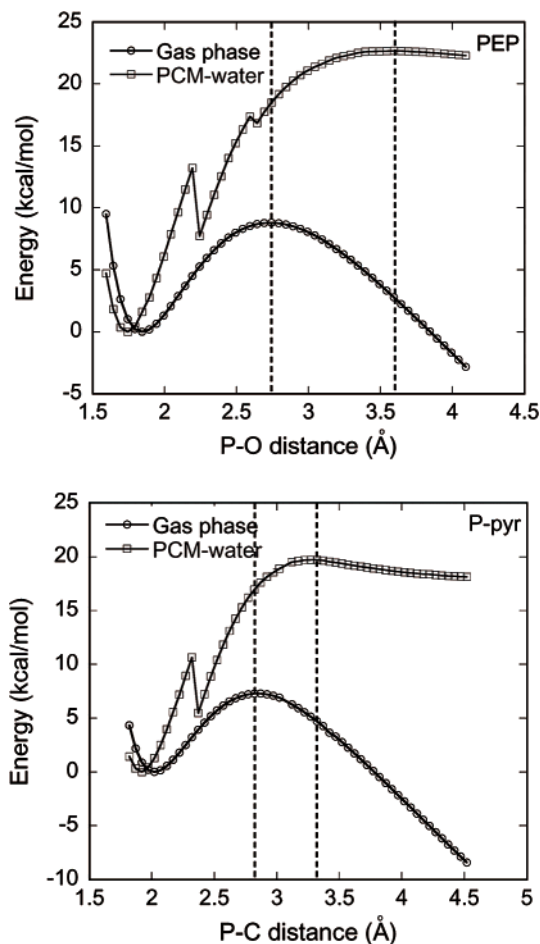*J. Phys. Chem. B, Vol. 109, No. 28, 2005* **13831**

Figure 4. Comparison of the minimal energy paths for the dissociation of PEP (upper panel) and P-pyr (lower panel) in the gas phase and in solution. The solution-phase curves were obtained using a constrained optimization method described in the text. The energy zero is defined at the equilibrium geometries, and the dashed lines are for the position of the barrier.
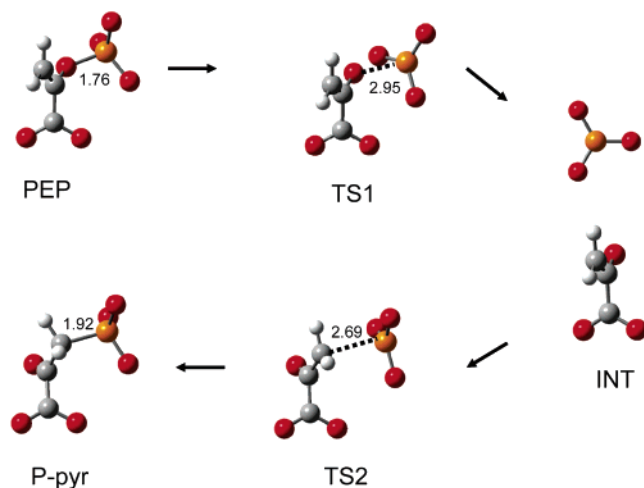

Figure 5. Stationary points for the solution-phase interconversion of PEP to P-pyr via the pyruvate enolate−metaphosphate intermediate obtained at the SCOSMO/MNDO/d level of theory.

0.08 Å to 2.69 Å at TS2. Other geometric changes are listed in Table 2. The corresponding dissociation free energy barrier height increases from 4.9 (10.0) kcal/mol in the gas phase to 18.6 (23.7) kcal/mol in solution for the cleavage of the P−O_3 (P−C_3) bond, again in reasonably good accord with the DFT

results. The differences seem to stem from the errors in the gas-phase MNDO/d results.

The increased activation barriers in the solution phase can at least partly be attributed to the charge distribution of the phosphoryl oxygen atoms. The Mulliken charges of these oxygen atoms in PEP ($-0.96e$, $-0.97e$, and $-1.0e$) are reduced at the transition state ($-0.83e$, $-0.84e$, and $-0.85e$), resulting in less solvation energy. Similar changes were also observed for the dissociation of P-pyr. Such charge reduction is a characteristic of the dissociative mechanism.[5]

Solvation also retards the Coulomb repulsion between the two charged intermediate species. The highly exothermic dissociation steps in the gas phase become endothermic events in solution. The endothermicity is consistent with the stability of PEP in water and further highlights the importance of solvation in such reactions. We note that the discussion of solvated metaphosphate is perhaps superficial, because its lifetime is known to be short in aqueous solution.[72−74] In PEP mutase, however, the evidence of its existence as a discrete intermediate is strong.

C. Thio Effects. The substitutions in both bridging and nonbridging oxygens of the phosphate group have been widely used in mechanistic investigations of phosphoryl transfer reactions.[43,45,46,61,75−77] For example, the observation of a large degree of racemization in the solvolysis of chiral *p*-nitrophenyl phosphorothioate indicated that the free thiometaphosphate could be the intermediate.[75] In this work, we focus on the thio effect for substitution of one nonbridging oxygen, motivated by recent work on the title reaction catalyzed by the PEP mutase.[30] Only DFT results are reported.

As shown in Table 3, the substitution increases the dissociation barrier for both the thio-substituted PEP and P-pyr (denoted as tPEP and tP-pyr) by 8−10 kcal/mol in the gas phase. However, in aqueous solution, the barriers for both dissociation processes are quite similar to the native (unsubstituted) systems. In particular, the activation barrier obtained from the solvated minimal energy path model is 20.6 (21.6) kcal/mol for the P−O_3 (P−C_3) bond cleavage, whereas the corresponding values for the native processes are 22.7 and 19.7 kcal/mol. The lower barrier for the P−O bond cleavage in the thio-substituted PEP is consistent with the experimental observation that the alkaline hydrolysis of *p*-nitrophenyl phosphorothioate is slightly faster than *p*-nitrophenyl phosphate,[76] in which the transition state is known to be dissociative.[78] In the enzymatic reaction, the conversion rates of both the oxo- and thio-PEP to the corresponding P-pyr products were also found to be similar,[30] which is consistent with our results.

The MNDO/d method was also employed to perform the geometry optimization in both the gas and the solution phases. In the gas phase, the agreement with the DFT barrier height for the dissociation of tPEP is quite good (18.6 vs 16.9 kcal/mol), but the MNDO/d barrier for the dissociation of tP-pyr (29.6 kcal/mol) is significantly higher than the B3LYP value (16.1 kcal/mol). The barriers for solution-phase reactions were found to be significantly larger than the B3LYP/PCM results, which can probably be attributed to the atomic radius of sulfur used in the SCOSMO calculations. To obtain a more quantitative agreement, this radius needs be recalibrated to measurable attributes such as pK_a for a well-sampled set of compounds.
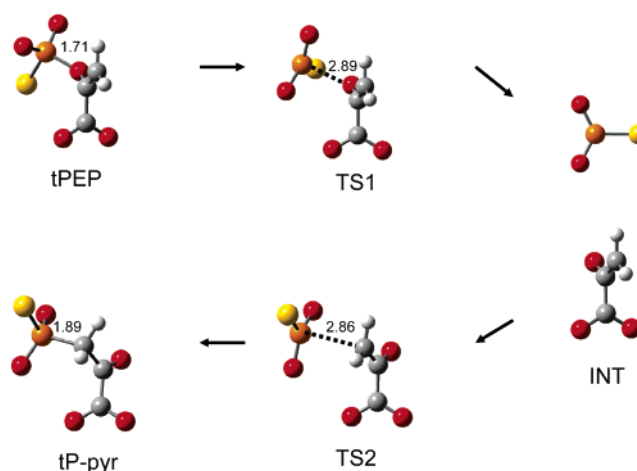
The optimized thio-substituted PEP stationary points obtained from the B3LYP and MNDO/d calculations are depicted in Figures 6 and 7, respectively, and the SCOSMO/MNDO/d structures in the solution phase are given in Figure 8. Some key geometrical properties are given in Table 4 for comparison.

13832 *J. Phys. Chem. B, Vol. 109, No. 28, 2005*

Xu et al.

TABLE 3: Energetics for Interconversion of Thio-Substituted PEP (tPEP) to Thio-Substituted P-pyr (tP-pyr) via the Pyruvate Enolate−Thiometaphosphate (INT)[a]

method	tPEP	TS1	INT	TS2	tP-pyr
$\Delta E_{gas(B3LYP/6-31++G(d,p))}$	0.0	16.42	−91.33	11.31	−6.08
$\Delta E_{gas(B3LYP/6-311++G(3df,2p)//B3LYP/6-31++G(d,p))}$	0.0	16.90	−92.34	12.88	−3.18
$\Delta G_{gas(B3LYP/6-311++G(3df,2p)//B3LYP/6-31++G(d,p))}$	0.0	13.17	−106.71	11.92	−2.52
$\Delta G_{gas} + \Delta G_{solv(PCM)}$ (single-point)	0.0	14.44	−9.36	18.95	2.18
$\Delta G_{gas} + \Delta G_{solv(COSMO)}$ (single-point)	0.0	12.05	−9.56	18.66	2.25
$\Delta E_{opt(PCM)}$ (estimated)	0.0	20.63		20.75	−0.82
$\Delta E_{gas(MNDO/d)}$	0.0	18.58	−90.26	20.90	−8.72
$\Delta G_{gas(MNDO/d)}$	0.0	17.15	−102.19	20.04	−9.02
$\Delta E_{opt(SCOSMO/MNDO/d)}$	0.0	34.52	31.75	36.78	−3.98
$\Delta G_{opt(SCOSMO/MNDO/d)}$	0.0	31.59	18.56	34.78	−4.68

[a] Energy units are given in kcal/mol.
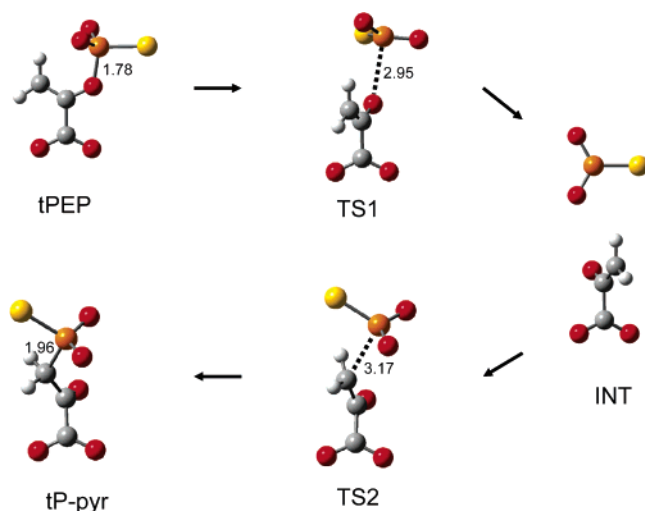
Figure 6. Stationary points for the gas-phase interconversion of tPEP to tP-pyr via the pyruvate enolate−thiometaphosphate intermediate obtained at the B3LYP/6-31++G(d,p) level of theory.
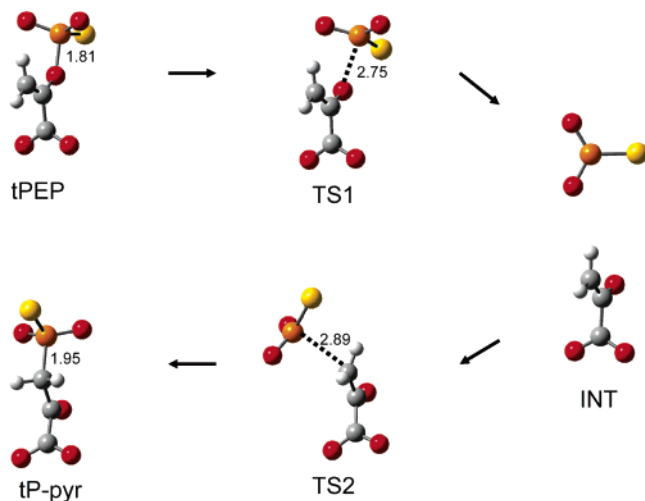
Figure 7. Stationary points for the gas-phase interconversion of tPEP to tP-pyr via the pyruvate enolate−thiometaphosphate intermediate obtained at the MNDO/d level of theory.

Figure 8. Stationary points for the solution-phase interconversion of tPEP to tP-pyr via the pyruvate enolate−thiometaphosphate intermediate obtained at the SCOSMO/MNDO/d level of theory.

TABLE 4: Geometries of Stationary Points for Interconversion of Thio-Substituted PEP (tPEP) to Thio-Substituted P-pyr (tP-pyr)[a]

method	d_1	d_2	d_3	d_4	φ[b]
			tPEP		
B3LYP/6-31++G(d,p)	1.7840	1.3490	1.3581	3.2076	163.4
MNDO/d	1.8120	1.3257	1.3714	3.4848	92.4
SCOSMO/MNDO/d	1.7103	1.3701	1.3533	3.6082	75.9
			TS1		
B3LYP/6-31++G(d,p)	2.9447	1.2868	1.3954	4.3642	66.4
MNDO/d	2.7467	1.2728	1.3969	4.5453	91.9
SCOSMO/MNDO/d	2.8944	1.2867	1.3744	4.9246	109.8
			TS2		
B3LYP/6-31++G(d,p)	5.0167	1.2765	1.4204	3.1695	74.8
MNDO/d	4.6291	1.2641	1.4211	2.8888	93.4
SCOSMO/MNDO/d	4.0338	1.2720	1.3946	2.8586	77.9
			tP-pyr		
B3LYP/6-31++G(d,p)	3.7127	1.2392	1.5102	1.9598	68.5
MNDO/d	3.3607	1.2328	1.5328	1.9463	88.9
SCOSMO/MNDO/d	3.5570	1.2316	1.5290	1.8848	68.1

[a] Bond lengths are given in angstroms, and angles are given in degrees. [b] φ is defined as the $O_1-C_1-C_2-O_3$ dihedral angle.

Like in the native PEP, the MNDO/d method gives similar geometries of tPEP with DFT except for the $O_1-C_1-C_2-O_3$ dihedral angle. Again, the MNDO/d approach found that the carboxylate and enol planes are nearly perpendicular in PEP, whereas the B3LYP geometry indicates that they are nearly parallel. As the system approaches TS1, the B3LYP angle changes by about 97.0°, but the change is negligible for MNDO/d. The agreement for the dihedral angle is much better for the dissociation of tP-pyr, in which the angle hardly changes from

tP-pyr to TS2. As shown in Table 4, solvation has a significant impact on the geometries of the stationary points, in a fashion similar to that observed in the native system. For instance, the $P-O_3$ bond in the solution phase is shortened in PEP while elongated in TS1.

Interesting issues about thio-substituted phosphates are the bond order and charge distribution of the nonbridging oxygen and sulfur. Due to the small electron negativity, it is tempting to conclude that the sulfur is less negatively charged than the

Studies of Dissociative Phosoryl Transfer

J. Phys. Chem. B, Vol. 109, No. 28, 2005 **13833**

oxygen. However, sulfur is also a "softer" ligand that can more readily accommodate a full formal negative charge than a "harder" oxygen. This is consistent with the observed lower pK_a values of thiols relative to the corresponding alcohols. Indeed, experimental evidence supports a more negatively charged sulfur atom, which forms a single bond with P.[79] This is confirmed by our calculations. The Mulliken charge of sulfur in the thio-substituted PEP is $-0.95e$, more negative than those for the two nonbridging oxygen atoms ($-0.81e$ and $-0.79e$). The bond order of the S−P bond is most likely single with a bond length of 2.11 Å. However, the O−P bonds have more double bond characteristics, as shown by the bond lengths of 1.53 and 1.52 Å.

IV. Discussion

The PEP-mutase-catalyzed conversion of PEP to P-pyr has an equilibrium constant of $\sim 10^{-3}$,[26,27] indicating a more stable PEP. Our calculated reaction free energy ΔG in solution, which is 3.67 (3.64) kcal/mol at the B3LYP/6-311++G(3df,2p) level with the PCM (COSMO) implicit solvent model, is consistent with the experimental value. The turnover rate for the formation of PEP is 5 s^{-1}, while that for the reverse reaction is 100 s^{-1}.[27] According to the transition state theory, the activation free energies for the enzymatic reaction are approximately 16 and 15 kcal/mol (assuming a unit transmission coefficient), respectively. By comparison with the calculated solution-phase barriers listed in Table 1, the rate enhancement of the enzyme is estimated to be on the order of $10^3 - 10^5$.

How does the enzyme achieve the catalytic efficiency? Given the small gas-phase barriers, it would be tempting to assume that the enzyme achieves that by desolvation. However, the active site of PEP mutase has an Mg^{2+} cofactor and several charged/polar residues, such as Asp58, Arg159, Asn122, and His190, and several water molecules. They apparently provide a favorable binding environment for the anionic PEP and P-pyr. Indeed, mutation of some such residues has been shown to lead to a larger K_m.[25,29] However, their role in catalysis is much less clear. The likely origin of the catalysis efficiency is the selective stabilization of the transition states by an preorganized electrostatic environment provided by relatively rigid charged residues in the active site. For instance, the Mg^{2+} ion may engage in strong interaction with the enol moiety during the dissociation of PEP,[80] while His190, Asn122, and Arg190 provides stabilization to the metaphosphate intermediate. A complete understanding of the catalytic strategy requires detailed simulations of the reaction potentials of mean force within the solvated protein environment.

In the absence of such elaborate investigations, the theoretical studies reported here can still provide valuable insights into the enzymatic reaction. The proposed dissociation mechanism[25] stipulates that the enol moiety undergoes rotation along the C$_1$−C$_2$ bond so that the metaphosphate from the dissociation of PEP can be reattached with C$_3$ to form P-pyr. Our theoretical results are in support of such a mechanism. Indeed, both HF and DFT structures for the pyruvate enolate intermediate show that the enol plane is essentially perpendicular to the carboxylate plane. Assuming that the carboxylate group is held in position by Mg^{2+}, the OH group of Ser46, and the backbone NH group of Leu48,[25] the metaphosphate should have easy access to both C$_3$ and O$_3$ for the formation of P−C and P−O bonds.

Interestingly, the PEP conformation deduced from the X-ray structure of the PEP mutase complexed with a P-pyr analogue (sulfopyruvate or S-pyr) indicates a 127.1° O$_1$−C$_1$−C$_2$−O$_3$ dihedral angle.[25] Such a twisted conformation was speculated

to maximize the interaction with Arg159 and His190. As shown in Figure 3, the carboxylate group is quite flexible, as shown by the small (0.8 kcal/mol) barrier at 90°. As a result, the energy penalty for the twisted C$_1$−C$_2$ bond is not expected to be severe. Indeed, similar twists in PEP have been noted in other enzyme−PEP complexes.[69,70]

V. Conclusions

In this work, we report a detailed investigation of an uncatalyzed phosphoryl transfer reaction that interconverts PEP to P-pyr. Our theoretical results indicate that both PEP and P-pyr dissociate via a barrier in the gas phase and in solution. Solvation is shown to substantially alter the geometry and energy of stationary points, due to the highly charged nature of the system. The most striking solvent effect is probably the retardation of the Coulomb repulsion between the anionic pyruvate enolate and the metaphosphate, which are vital in rendering both PEP and P-pyr stable in aqueous solution. The substitution of a nonbridging phosphoryl oxygen by sulfur is shown to result in significant changes in the gas-phase energies. However, the so-called thio effect is small for solution reactions. The latter conclusion is consistent with several experimental observations.

The geometries of stationary points provide strong support of the proposed dissociative mechanism for the enzyme-catalyzed rearrangement of PEP to P-pyr. In particular, it is shown that the enol plane rotates relative to the carboxylate plane as the P−O bond of PEP cleaves. The resulting pyruvate enolate intermediate features an enol plane facing the metaphosphate, allowing the formation of the P−C$_3$ bond and thus the P-pyr product. In addition, the carboxylate group is shown to be quite free to rotate along the C$_1$−C$_2$ axis in PEP, thus providing a reasonable explanation for the twisted PEP structure observed in the enzyme−substrate complex. The theoretical work reported here lays a solid foundation for future QM/MM studies of the enzymatic reaction, which are expected to elucidate the role played by the metal cofactor and active-site residues in stabilizing the transition states.

The semiempirical MNDO/d method produces results that are in reasonably good agreement with the DFT treatment. The agreement is better for the dissociation of the P−O bond. The larger discrepancies in the P-pyr dissociation channel, particularly for the thio-substituted P-pyr, could be due to the undersampling of phosphonates in the original parametrization. To achieve quantitative agreement, a set of special reaction parameters (SRP) will need to be developed for this reaction. This will be important for an accurate QM/MM description of the enzymatic reaction.

The SCOSMO method provides a powerful method to study solvent effects, because it allows stable geometric optimization of solvated species. It is very encouraging that the results for the native reaction are in satisfactory agreement with the DFT/PCM model. The overestimation of the reaction barriers in the thio-substituted system can be attributed to the van der Waals radius of sulfur, which needs to be recalibrated.

Xu et al.

Supporting Information Available: Cartesian coordinates of all the stationary points. This material is available free of charge via the Internet at http://pubs.acs.org.

References and Notes

(1) Westheimer, F. H. *Science* **1987**, *235*, 1173.

(2) Mildvan, A. S. *Proteins* **1997**, *29*, 401.

(3) Benkovic, S. J.; Schray, K. J. Mechanisms of phosphoryl transfer. In *Transition States of Biochemical Processes*; Gandour, R. D., Ed.; Plenum: New York, 1978.

(4) Thatcher, G. R. J.; Kluger, R. *Adv. Phys. Org. Chem.* **1989**, *25*, 99.

(5) Admiraal, S. J.; Herschlag, D. *Chem. Biol.* **1995**, *2*, 729.

(6) Knowles, J. R. *Annu. Rev. Biochem.* **1980**, *49*, 877.

(7) Hengge, A. C. Transfer of the PO_3^{2-} group. In *Comprehensive Biological Catalysis*; Sinnot, M., Ed.; Academic Press: San Diego, CA, 1998; Vol. 1.

(8) Allen, K. N.; Dunaway-Mariano, D. *Trends Biochem. Sci.* **2004**, *29*, 495.

(9) Florian, J.; Warshel, A. *J. Phys. Chem. B* **1998**, *102*, 719.

(10) Hu, C.-H.; Brinck, T. *J. Phys. Chem. A* **1999**, *103*, 5379.

(11) Bianciotto, M.; Barthelat, J.-C.; Vigroux, A. *J. Am. Chem. Soc.* **2002**, *124*, 7573.

(12) Bianciotto, M.; Barthelat, J.-C.; Vigroux, A. *J. Phys. Chem. A* **2002**, *106*, 6521.

(13) Wang, Y.-N.; Topol, I. A.; Collins, J. R.; Burt, S. K. *J. Am. Chem. Soc.* **2003**, *125*, 13265.

(14) Herschlag, D.; Jencks, W. P. *J. Am. Chem. Soc.* **1987**, *109*, 4665.

(15) Herschlag, D.; Jencks, W. P. *J. Am. Chem. Soc.* **1989**, *111*, 7587.

(16) Kim, K.; Cole, P. A. *J. Am. Chem. Soc.* **1997**, *119*, 11096.

(17) Kim, K.; Cole, P. A. *J. Am. Chem. Soc.* **1998**, *120*, 6851.

(18) Choe, J.-Y.; Iancu, C. V.; Fromm, H. J.; Honzatko, R. B. *J. Biol. Chem.* **2003**, *278*, 16015.

(19) Bowman, E.; McQueney, M.; Barry, R. J.; Dunaway-Mariano, D. *J. Am. Chem. Soc.* **1988**, *110*, 5575.

(20) Seidel, H. M.; Freeman, S.; Seto, H.; Knowles, J. R. *Nature* **1988**, *335*, 457.

(21) Seidel, H. M.; Freeman, S.; Schwalbe, C. H.; Knowles, J. R. *J. Am. Chem. Soc.* **1990**, *112*, 8149.

(22) Seto, H.; Kuzuyama, T. *Nat. Prod. Rep.* **1999**, *16*, 589.

(23) Masterlerz, P. In *Natural Products Chemistry*; Zulewski, R., Skolik, J. J., Eds.; Elsevier: Amsterdam, The Netherlands, 1984.

(24) Huang, K.; Li, Z.; Jia, Y.; Dunaway-Mariano, D.; Herzberg, O. *Structure* **1999**, *7*, 539.

(25) Liu, S.; Lu, Z.; Jia, Y.; Dunaway-Mariano, D.; Herzberg, O. *Biochemistry* **2002**, *41*, 10270.

(26) Seidel, H. M.; Knowles, J. R. *Biochemistry* **1994**, *33*, 5641.

(27) Kim, J.; Dunaway-Mariano, D. *Biochemistry* **1996**, *35*, 4628.

(28) Kim, A.; Kim, J.; Martin, B. M.; Dunaway-Mariano, D. *J. Biol. Chem.* **1998**, *273*, 4443.

(29) Jia, Y.; Lu, Z.; Huang, K.; Herzberg, O.; Dunaway-Mariano, D. *Biochemistry* **1999**, *38*, 14165.

(30) McQueney, M. S.; Lee, S.-L.; Swartz, W. H.; Ammon, H. L.; Mariano, P. S.; Dunaway-Mariano, D. *J. Org. Chem.* **1991**, *56*, 7121.

(31) Warshel, A. *Computer Modeling of Chemical Reactions in Enzymes and Solutions*; Wiley: New York, 1991.

(32) Garcia-Viloca, M.; Gao, J.; Karplus, M.; Truhlar, D. G. *Science* **2004**, *303*, 186.

(33) Warshel, A.; Levitt, M. *J. Mol. Biol.* **1976**, *103*, 227.

(34) Singh, U. C.; Kollman, P. A. *J. Comput. Chem.* **1986**, *7*, 718.

(35) Field, M. J.; Bash, P. A.; Karplus, M. *J. Comput. Chem.* **1990**, *11*, 700.

(36) Gao, J. *Acc. Chem. Res.* **1996**, *29*, 298.

(37) Thiel, W.; Voityuk, A. A. *J. Phys. Chem.* **1996**, *100*, 616.

(38) Lopez, X.; York, D. M. *Theor. Chem. Acc.* **2003**, *109*, 149.

(39) Dejaegere, A.; Karplus, M. *J. Am. Chem. Soc.* **1993**, *115*, 5316.

(40) Florian, J.; Warshel, A. *J. Am. Chem. Soc.* **1997**, *119*, 5473.

(41) Chang, N.-y.; Lim, C. *J. Am. Chem. Soc.* **1998**, *120*, 2156.

(42) Lopez, X.; Dejaegere, A.; Karplus, M. *J. Am. Chem. Soc.* **2001**, *123*, 11755.

(43) Gregersen, B. A.; Lopez, X.; York, D. M. *J. Am. Chem. Soc.* **2004**, *126*, 7504.

(44) Range, K.; McGrath, M. J.; Lopez, X.; York, D. M. *J. Am. Chem. Soc.* **2004**, *126*, 1654.

(45) Breslow, R.; Katz, I. *J. Am. Chem. Soc.* **1968**, *90*, 7376.

(46) Herschlag, D.; Piccirilli, J. A.; Cech, T. R. *Biochemistry* **1991**, *30*, 4844.

(47) Miertus, S.; Scrocco, E.; Tomasi, J. *Chem. Phys.* **1981**, *55*, 117.

(48) Miertus, E.; Tomasi, J. *Chem. Phys.* **1982**, *65*, 239.

(49) Barone, V.; Cossi, M. *J. Phys. Chem. A* **1998**, *102*, 1995.

(50) York, D. M.; Karplus, M. *J. Phys. Chem. A* **1999**, *103*, 11060.

(51) Khandogin, J.; Gregersen, B. A.; Thiel, W.; York, D. M. *J. Phys. Chem. B* **2005**, *109*, 9799.

(52) Gregersen, B. A.; Khandogin, J.; Thiel, W.; York, D. M. *J. Phys. Chem. B* **2005**, *109*, 9810.

(53) Benkovic, S. J.; Schray, K. J. *Biochemistry* **1968**, *7*, 4090.

(54) Freeman, S.; Irwin, W. J.; Schwalbe, C. H. *J. Chem. Soc., Perkin Trans. 2* **1991**, 263.

(55) Frisch, M. J.; Trucks, G. W.; Schlegel, H. B.; Scuseria, G. E.; Robb, M. A.; Cheeseman, J. R.; Montgomery, Jr., J. A.; Vreven, T.; Kudin, K. N.; Burant, J. C.; Millam, J. M.; Iyengar, S. S.; Tomasi, J.; Barone, V.; Mennucci, B.; Cossi, M.; Scalmani, G.; Rega, N.; Petersson, G. A.; Nakatsuji, H.; Hada, M.; Ehara, M.; Toyota, K.; Fukuda, R.; Hasegawa, J.; Ishida, M.; Nakajima, T.; Honda, Y.; Kitao, O.; Nakai, H.; Klene, M.; Li, X.; Knox, J. E.; Hratchian, H. P.; Cross, J. B.; Bakken, V.; Adamo, C.; Jaramillo, J.; Gomperts, R.; Stratmann, R. E.; Yazyev, O.; Austin, A. J.; Cammi, R.; Pomelli, C.; Ochterski, J. W.; Ayala, P. Y.; Morokuma, K.; Voth, G. A.; Salvador, P.; Dannenberg, J. J.; Zakrzewski, V. G.; Dapprich, S.; Daniels, A. D.; Strain, M. C.; Farkas, O.; Malick, D. K.; Rabuck, A. D.; Raghavachari, K.; Foresman, J. B.; Ortiz, J. V.; Cui, Q.; Baboul, A. G.; Clifford, S.; Cioslowski, J.; Stefanov, B. B.; Liu, G.; Liashenko, A.; Piskorz, P.; Komaromi, I.; Martin, R. L.; Fox, D. J.; Keith, T.; Al-Laham, M. A.; Peng, C. Y.; Nanayakkara, A.; Challacombe, M.; Gill, P. M. W.; Johnson, B.; Chen, W.; Wong, M. W.; Gonzalez, C.; Pople, J. A. *Gaussian 03*, revision C.02; Gaussian, Inc.: Wallingford, CT, 2004.

(56) Becke, A. D. *J. Chem. Phys.* **1993**, *98*, 5648.

(57) Lee, C.; Yang, W.; Parr, R. G. *Phys. Rev. B* **1988**, *37*, 785.

(58) Lopez, C. S.; Faza, O. N.; Gregersen, B. A.; Lopez, X.; de Lera, A. R.; York, D. M. *ChemPhysChem* **2004**, *5*, 1045.

(59) Gonzalez, C.; Schlegel, H. B. *J. Chem. Phys.* **1989**, *90*, 2154.

(60) Gonzalez, C.; Schlegel, H. B. *J. Phys. Chem.* **1990**, *94*, 5523.

(61) Gregersen, B. A.; Lopez, X.; York, D. M. *J. Am. Chem. Soc.* **2003**, *125*, 7178.

(62) Xie, D.; Zhou, Y.; Xu, D.; Guo, H. *Org. Lett.* **2005**, *7*, 2093.

(63) Barone, V.; Cossi, M.; Tomasi, J. *J. Chem. Phys.* **1997**, *107*, 3210.

(64) Bondi, A. *J. Phys. Chem.* **1964**, *68*, 441.

(65) Hayes, D. M.; Kenyon, G. L.; Kollman, P. A. *J. Am. Chem. Soc.* **1978**, *100*, 4332.

(66) Schwalbe, C. H.; Freeman, S. *J. Chem. Soc., Chem. Commun.* **1990**, 251.

(67) Weichsel, A.; Lis, T. *Acta Crystallogr., Sect. C* **1990**, *46*, 962.

(68) Souhassou, M.; Schaber, P. M.; Blessing, R. H. *Acta Crystallogr., Sect. B* **1996**, *52*, 865.

(69) Shumilin, I. A.; Bauerle, R.; Kretsinger, R. H. *Biochemistry* **2003**, *42*, 3766.

(70) Konig, V.; Pfeil, A.; Braus, G. H.; Schneider, T. R. *J. Biol. Chem.* **2004**, *337*, 675.

(71) Herzberg, O.; Chen, C. C. H.; Liu, S.; Tempczyk, A.; Howard, A.; Wei, M.; Ye, D.; Dunaway-Mariano, D. *Biochemistry* **2002**, *41*, 780.

(72) Herschlag, D.; Jencks, W. P. *J. Am. Chem. Soc.* **1989**, *111*, 7579.

(73) Wu, Y.-D.; Houk, K. N. *J. Am. Chem. Soc.* **1993**, *115*, 11997.

(74) Ma, B.; Xie, Y.; Shen, M.; Schleyer, P. v. R.; Schaefer, H. F., III *J. Am. Chem. Soc.* **1993**, *115*, 11169.

(75) Cullis, P. M.; Iagrossi, A. *J. Am. Chem. Soc.* **1986**, *108*, 7870.

(76) Catrina, I. E.; Hengge, A. C. *J. Am. Chem. Soc.* **1999**, *121*, 2156.

(77) Catrina, I. E.; Hengge, A. C. *J. Am. Chem. Soc.* **2003**, *125*, 7546.

(78) Hengge, A. C.; Edens, W. A.; Elsing, H. *J. Am. Chem. Soc.* **1994**, *116*, 5045.

(79) Frey, P. A.; Sammons, R. D. *Science* **1985**, *228*, 541.

(80) Benkovic, S. J.; Schray, K. J. *Biochemistry* **1968**, *7*, 4097.